Quantum Information Processing (2024) 23:256
https://doi.org/10.1007/s11128-024-04465-z

Exploiting OFDM method for quantum communication

Abdulbasit M. A. Sabaawi[1,2] · Mohammed R. Almasaoodi[1,3] · Sándor Imre[1]

Received: 1 March 2024 / Accepted: 12 June 2024
© The Author(s) 2024

Abstract
Orthogonal frequency-division multiplexing (OFDM) is a crucial modulation method used in contemporary digital communication systems for its significant spectral efficiency, low latency, and robustness in challenging environments. This work examines the novel use of OFDM in quantum communication, an area that offers exceptional security and efficiency in information transfer using quantum mechanics principles. In the rapidly evolving field of quantum computing, understanding, and mitigating quantum bit errors is paramount. This paper presents a rigorous analysis of bit error rates (BER) in quantum circuits, focusing on the impact of the quantum Fourier transform and its inverse, contrasted against quantum circuits employing dynamic gate sequences. Our research methodology encompasses simulations over a diverse set of parameters, including varying qubit counts ranging from 2 to 8 and theta angles (15, 30, 45, and 60°), as well as random theta values, utilizing the advanced capabilities of the Qiskit framework. Our findings indicate that quantum OFDM substantially improves quantum communication, lowering errors and boosting security. The quantum model outperforms the reference model in BER, with further enhancements as qubits increase.

Keywords Bit error rate · Orthogonal frequency division multiplexing · Quantum communication · Quantum Fourier transform

✉ Abdulbasit M. A. Sabaawi
abdulbasit@hit.bme.hu

Mohammed R. Almasaoodi
Almasaoodi@hit.bme.hu

Sándor Imre
imre@hit.bme.hu

1 Department of Networked Systems and Services, Faculty of Electrical Engineering, and Informatics, Budapest University of Technology and Economics, Budapest, Hungary

2 College of Electronics Engineering, Ninevah University, Mosul, Iraq

3 Kerbala University, Kerbala, Iraq

Published online: 26 June 2024

1 Introduction

Quantum communication represents a significant advancement in secure communication, utilizing the fundamental principles of quantum mechanics, such as quantum entanglement and superposition, to greatly enhance the method and security of transmitting information [1–4]. Quantum communication exploits the unique characteristics of quantum states to revolutionize communication technology, providing unprecedented levels of security and efficiency. Quantum entanglement enables the immediate transmission of quantum states between particles that are far apart, which has the potential to provide safe and real-time communication over vast distances [5, 6]. At the same time, the concept of quantum superposition—the idea that a quantum entity can be in more than one state at the same time—marks the beginning of communication channels that can handle much more information [7–9]. The fundamental principles of quantum mechanics form the basis of quantum communication, which drives the development of advanced technologies like quantum key distribution (QKD). QKD has the potential to achieve encryption that is theoretically impossible to break [10–14].

Significant advancements have been made in this field, particularly with the introduction of satellite-based quantum communication projects that seek to create quantum networks across great distances. The current research and development in quantum communication is set to usher in a new era of secure communication, establishing the foundational framework for the establishment of a quantum internet. This emerging discipline is on the verge of reshaping the landscape of secure communication, with the ability to create a secure communication infrastructure based on the unchanging principles of quantum mechanics[15, 16].

Following the advancements in quantum communication, the role of error correction becomes crucial due to the delicate nature of quantum states. Since noise can easily disrupt these states, error correction is essential for maintaining the integrity of quantum information over long distances[17]. Quantum error correction techniques are designed to protect this information from errors without disturbing the quantum state itsel f [18]. This research focuses on BER analysis and reduction in quantum communication, an area concomitantly connected with quantum error correction advancements. Notably, innovative encoding methods [19] and the development of deep quantum error decoders [20] directly contribute to BER reduction, enhancing communication reliability. This study underscores the crucial interplay between BER reduction efforts and quantum error correction strategies, aiming to improve quantum communication fidelity and integrity.

Orthogonal frequency-division multiplexing (OFDM) is a fundamental technique employed in a communication system to effectively address problems such as signal fading and interference. This process involves the partitioning of a signal into several closely positioned channels, enabling the simultaneous transmission of data across them. OFDM is highly advantageous for digital TV, wireless internet, and other high-speed data services because of its ability to rapidly and accurately convey data[21, 22]. OFDM significantly influences the bit error rate (BER) in communication systems by mitigating wireless channel impairments such as multipath fading and inter-symbol interference (ISI) [23, 24]. OFDM's strategy of dividing the broadband channel into

multiple orthogonal narrowband sub-channels efficiently reduces ISI, facilitating high data rate transmissions with optimized spectrum utilization. This makes OFDM a preferred technology in modern wireless communication systems, where maintaining a low BER is essential for achieving reliable and efficient data transmission [25]. The OFDM technique's ability to deal with imperfect channels also suggests it could be useful in quantum communication, offering a way to improve the reliability of quantum networks.

Quantum orthogonal frequency-division multiplexing (Q-OFDM) adapts traditional OFDM techniques to quantum communication to potentially reduce qubit errors. Q-OFDM tries to improve communication reliability against noise and decoherence by encoding quantum information across multiple frequencies. This is a big step towards making quantum networks work better.

Q-OFDM employs the quantum Fourier transform (QFT) and its inverse (IQFT) to encode and decode data delivered across quantum communication channels. QFT is one of the most important key components in quantum algorithms [26]. Its value of this technology lies in its capability to identify periodic structures of quantum states, upon which many quantum algorithms depend to obtain a demonstrable superiority over conventional algorithms. For instance, Shor's algorithm [27] efficiently factors large integers, phase estimation [28] is used in simulations of quantum systems, and there are many other applications. In the realm of quantum communication, many researchers have employed QFT in several advanced applications. Examples of these applications include quantum sensing [29], quantum teleportation [30], and quantum repeaters [31]. On the other hand, IQFT is essentially the reverse process of the QFT. While the QFT maps a quantum state from the time domain to the frequency domain, the IQFT performs the opposite, converting a state from the frequency domain back to the time domain. Quantum computing relies heavily on this, especially in algorithms that require the conversion of QFT output into a more comprehensible form, like Shor's factoring algorithm. The IQFT uses a similar process as the QFT but with inverse phase rotations, allowing for the reconstruction of the original quantum state.

Numerous studies have underscored the pivotal role of the QFT and IQFT in advancing quantum computing. The findings from these investigations reveal the potential to enhance error correction, communication protocols, and more, thereby increasing the applicability of quantum technologies across various scientific domains. The study [32], presented a multi-user quantum communication system that integrates code division multiple access (CDMA) with both QFT and IQFT. Their approach improves scalability and security, enabling simultaneous communication among multiple users while resisting eavesdropping. In [33], the authors introduced a novel quantum teleportation protocol leveraging the QFT. The protocol allows for the efficient teleportation of arbitrary quantum states by employing QFT and IQFT for encoding and decoding information. This method simplifies and improves the accuracy of the teleportation process, demonstrating the potential of optimized QFT and IQFT to enhance quantum communication protocols. The authors in [34] enhanced the quantum phase estimation (QPE) algorithm by optimizing the use of QFT and IQFT. Their approach reduces circuit depth and error rates, leading to improved accuracy and efficiency in QPE. By

benchmarking their method against existing implementations, they demonstrate significant improvements, highlighting the crucial role of optimized QFT and IQFT in effective quantum computing applications.

On the other hand, researchers have used the integration of OFDM with quantum technology, which has emerged as a groundbreaking approach. In [35], the authors introduced an approach to quantum key distribution (QKD) by incorporating OFDM, a technique widely used in classical communication systems, to enhance the performance and security of QKD systems. This integration aims to address key challenges in QKD, such as system imperfections and time misalignment, by leveraging OFDM's spectral efficiency. In the context of quantum communication, QKD offers a theoretically secure framework for exchanging cryptographic keys between parties. The integration of OFDM into QKD represents a significant advancement by potentially increasing the robustness and capacity of quantum networks. The paper considers real-world imperfections that could affect the system's integrity and reliability. The authors in [36], proposed a new method by combining IF-Over-Fiber transmission with OFDM and quantum noise to improve physical layer encryption. By integrating quantum mechanics principles with OFDM, this research provides a fresh perspective on enhancing wireless network security. It fills a gap in current encryption techniques, promising better security for data transmission in an increasingly digital world. In [37], the authors explored the innovative intersection of quantum computing with telecommunications to enhance 5G and IoT capabilities, specifically within healthcare. By integrating quantum computing principles with OFDM signal processing, this study presented a theoretical and practical framework that promises significant improvements in data transmission rates, reliability, and security for healthcare applications. In [38], the authors suggested a technique of encryption by integrating quantum noise with DFT-spread OFDM technology, aiming to significantly enhance communication security. This method leverages the unpredictability of quantum noise to strengthen the encryption of data transmissions, offering a robust defense against the potential threats posed by quantum computing. The study simulations demonstrate the system effectiveness, suggesting it is a promising solution for future-proofing digital communications against advanced decryption techniques. In [39], the authors introduced a novel approach to enhance resource allocation in cognitive radio networks. By integrating Quantum particle swarm optimization (QPSO) with radial basis function (RBF) neural networks, the study proposes a hybrid model that optimizes network performance in overlay cognitive OFDM systems. This method significantly improves spectral efficiency and throughput, ensuring minimal interference with primary users. Highlighting the efficacy of combining quantum-inspired algorithms with machine learning for complex optimization challenges.

In synthesizing the extant literature on the advent of OFDM in quantum paradigms, the present research endeavors to pioneer the conceptualization and application of quantum OFDM. This initiative seeks to delineate and amplify the utility of OFDM methodologies within the quantum communication landscape, thereby advancing the theoretical and practical integration of these 2 domains.

This study considers using the quantum OFDM system (Q-OFDM), specifically focusing on the calculation of BER across varying numbers of qubits and different types of channels, with a particular focus on channels characterized by randomized

rotations (utilizing R_x and R_y gates). By integrating quantum communication, the study aims to assess how quantum properties can influence the BER in a Q-OFDM system. The theoretical integration of quantum principles with OFDM could potentially revolutionize error minimization strategies in quantum communication systems. This integration aims to harness quantum mechanics' inherent parallelism and noise resistance to improve data transmission's reliability and efficiency across quantum channels. The study looks at different quantum situations, including the use of the quantum Fourier transform (QFT) and the inverse quantum Fourier transform (IQFT) as signal multiplexing methods. It considers how changes in the number of qubits and the nature of quantum channels can affect the performance and reliability of OFDM systems in quantum computing.

The structure of this paper is as follows: Sect. 2 presents a comprehensive quantum OFDM transmission model that is realized using QFT/IQFT. The results in Sect. 3 demonstrate the variation of the bit error rate (BER) across various channel types and qubit quantities. Section 4 offers a definitive review of the research's results and consequences.

2 Quantum OFDM model

We introduce an innovative method denoted as quantum orthogonal frequency division multiplexing (Q-OFDM), which exploits the principles of the quantum Fourier transform (QFT) and its inverse (IQFT) to facilitate the encoding and decoding of data transmitted through quantum communication channels, as depicted in Fig. 1. This methodology draws inspiration from its classical counterpart, OFDM, which utilizes a spectrum of orthogonal carrier frequencies to convey information across a medium. Within the quantum framework, the QFT is employed to generate a state of superposition that emulates these carrier frequencies, whereby each quantum state has the potential to transport an individual qubit of data.

The exposition begins with a detailed examination of the quantum encoder's operation. Commencing with a superposition state $|\psi\rangle$ within the computational basis vector space, this construct serves as the foundational architecture. Herein, data bits,

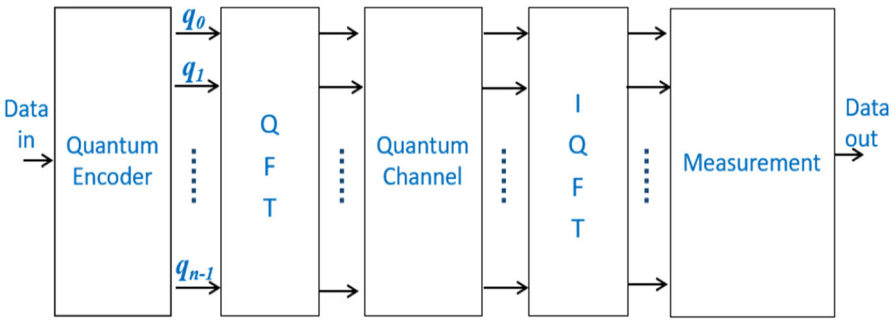

Fig. 1 The quantuam OFDM model

identified as M, undergo a transformation process culminating in a quantum state that spans n qubits, delineated in the subsequent equation,

$$|\psi\rangle = \sum_{i=0}^{N-1} \psi_i |i\rangle \tag{1}$$

This equation characterizes the initial quantum state as an aggregate of basis states $|i\rangle$, where each coefficient ψ_i corresponds to the amplitude of the associated basis state within the superposition. N signifies the sum of unique outcomes from n bits, expressed as $N = 2^n$.

The complete set of message bits, M, is contained within a single quantum register whose size matches $\log_2(M)$. This encoded state, $|\psi\rangle$, is subsequently termed the modulated quantum message or register. The transformation is applied as $|\psi_{trans}\rangle = \mathrm{Q}FT|\psi\rangle$.

2.1 Introduction to quantum Fourier transform

The Fourier transform is a pivotal instrument in classical computing, applied extensively across areas such as signal processing and complexity theory. Its quantum counterpart, the quantum Fourier transform (QFT), modifies this concept for use in quantum computing by altering the probability amplitudes of quantum states. Serving as a crucial element in numerous quantum algorithms, the QFT is instrumental in processes like Shor's algorithm for factorization and methods for quantum phase estimation [40, 41].

The classical discrete Fourier Transform (DFT) operates on a sequence of complex numbers $x0, x1, \ldots, xN-1$, transforming this sequence into a new series $y0, y1, \ldots, yN-1$, as delineated by the following relationship,

$$y_k = \frac{1}{\sqrt{N}} \sum_{j=0}^{N-1} x_j \omega_N^{jk} \tag{2}$$

In this expression, ω_N represents the N^{th} root of unity, given by $\omega_N = e^{\frac{2\pi i}{N}}$.

Simultaneously, the QFT acts upon a quantum state $|X\rangle = \sum_{j=0}^{N-1} x_j |j\rangle$, transforming it into another quantum state $|Y\rangle = \sum_{k=0}^{N-1} y_k |k\rangle$, where the coefficients yk align with the discrete Fourier transform's output, as shown in Eq. (2). This specialized transformation uniquely adjusts the probability amplitudes within the quantum state.

It is critical to note that this transformation specifically targets the amplitude probabilities of the quantum state for modification.

Moreover, this process can be conceptualized as a mapping where each basis state $|j\rangle$ is mapped to:

$$|j\rangle \rightarrow \frac{1}{\sqrt{N}} \sum_{k=0}^{N-1} \omega_N^{-jk} |k\rangle \tag{3}$$

This framework can also be shown by making a unitary matrix, which encapsulates the transformation's essence in a linear algebraic format that keeps the quantum state's norm and lets amplitudes be interpreted in terms of probability[13].

$$U_{QFT} = \frac{1}{\sqrt{N}} \sum_{j=0}^{N-1} \sum_{k=0}^{N-1} \omega_N^{-jk} |k\rangle\langle j| \tag{4}$$

2.2 Implementation of quantum Fourier transform

The QFT is a crucial mechanism in quantum computing, bridging the gap between the computational (or Z) basis and the Fourier basis, 2 integral frameworks within the field. The Hadamard gate (H-gate), which represents the QFT applied to a single qubit, facilitates the transition from the computational basis states $|0\rangle$ and $|1\rangle$ to the X-basis states $|+\rangle$ and $|-\rangle$, respectively. This concept is scalable to systems of multiple qubits, wherein each state defined within the computational basis finds a counterpart in the Fourier basis, underscoring the QFT's role in enabling this foundational basis conversion [42].

$$\mathrm{QFT}|z\rangle = |\tilde{z}\rangle. \tag{5}$$

States in the Fourier basis are frequently distinguished by appending a tilde symbol (~) above the state, to demarcate them from their equivalents in the computational basis. This expression delineates the QFT's function in translating between these critical bases, underlining its essential contribution to quantum computing's operational versatility. Within the realm of quantum computation, numerical values are encoded utilizing the binary system, facilitated by the use of quantum bits, or qubits. These qubits possess the unique capability to be in a superposition of states, specifically $|0\rangle$ and $|1\rangle$.

The interaction of qubits with numerical increments is particularly intriguing. For example, $qubit3$ exhibits a state change with each increment, showcasing a straightforward binary progression. Conversely, $qubit2$ undergoes state changes every 2 increments, $qubit1$ every four, and $qubit0$ every eight, illustrating an exponential correlation to their respective positions. This behavior underscores the quantum principles of entanglement and interference, which are pivotal to the functionality of quantum computing.

In the domain of quantum information theory, numerical data intended for encoding is transformed into precise rotations of qubits around the Z-axis within the quantum state space, depicted by the Bloch sphere. As illustrated in the Fig. 2, within the state $|\widetilde{0}\rangle$, all qubits, from q_0, q_1, q_2 to q_3 are initialized in the state $|+\rangle$.

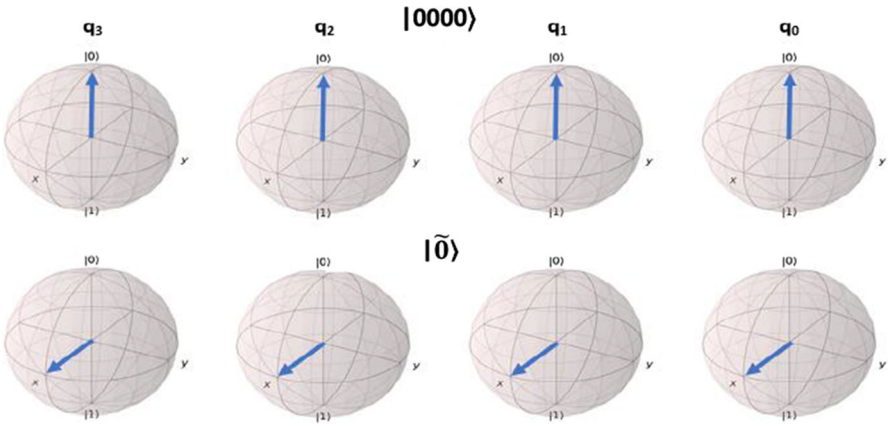

Fig. 2 The upper row depicts Bloch spheres for the quantum state |0000⟩. The lower row shows the resultant state after applying QFT on |0000⟩, represented as $|\widetilde{0}\rangle$

This encoding methodology emphasizes the differential rate at which the state transitions occur among the qubits: notably, the leftmost qubit (qubit 3) manifests the least frequent alterations, with every numerical increment prompting a flip between its states. Conversely, the rightmost qubit undergoes the most rapid state changes, flipping states with the minutest numerical increments attributable to its elevated binary significance. This planned strategy shows how qubits move in a quantum computing framework using binary-weighted dynamics, which is similar to the main ideas behind quantum superposition and phase encoding.

Exploring the QFT for an expanded state space, particularly where $N = 2^n$, highlights its enhanced effectiveness. Applied to a quantum state $|z\rangle = |z_1 \dots z_n\rangle$ as the most significant bit, the utility of the QFT becomes increasingly apparent. The application of the QFT to $|z\rangle$ can be represented as follows:

$$\text{QFT}|z\rangle = \frac{1}{\sqrt{N}} \sum_{y=0}^{N-1} \omega_N^{zy} |y\rangle. \tag{6}$$

In this expression, ω_N represents the Nth root of unity, given by $\omega_N = e^{\frac{2\pi i}{N}}$.

$$\text{QFT}|z\rangle = \frac{1}{\sqrt{2^n}} \sum_{y=0}^{2^n-1} e^{\frac{2\pi i z y}{2^n}} |y\rangle. \tag{7}$$

By expressing y in binary as $y = y_1 \dots y_n$ and substituting $2^n = \sum_{k=1}^{n} y_k 2^{n-k}$, the formula refines to:

$$\mathrm{QFT}|z\rangle = \frac{1}{\sqrt{2^n}} \sum_{y_1=0}^{1} \cdots \sum_{y_n=0}^{1} \prod_{k=1}^{n} e^{\frac{2\pi i z y_k}{2^k}} |y_1 \ldots y_n\rangle. \tag{8}$$

After some rearrangement and simplification, this results in:

$$QFT|z\rangle = \bigotimes_{k=1}^{n} \left(|0\rangle + e^{\frac{2\pi i z}{2^k}} |1\rangle \right) \tag{9}$$

Finally, when breaking down the summation, we can write this as:

$$\mathrm{QFT}|z\rangle = \frac{1}{\sqrt{2^n}} \left(|0\rangle + e^{\frac{2\pi i z}{2}} |1\rangle \right) \otimes \ldots \otimes \left(|0\rangle + e^{\frac{2\pi i z}{2^n}} |1\rangle \right) \tag{10}$$

These equations mathematically capture the previously discussed concepts, providing a clear link between intuitive understanding and formal mathematical representation.The QFT circuit is constructed from 2 fundamental gate types. The first gate, the single-qubit Hadamard gate (H), is ubiquitous in quantum computing. Its action on a qubit state $|z_k\rangle$ is described as:

$$H|z_k\rangle = \frac{1}{\sqrt{2}} \left(|0\rangle + e^{\frac{i\pi z_k}{2}} |1\rangle \right) \tag{11}$$

Following the Hadamard gate, the circuit utilizes the controlled rotation gate, $CROT_k$, which is depicted as a block-diagonal matrix:

$$CROT_k = \begin{bmatrix} I & 0 \\ 0 & UROT_k \end{bmatrix} \tag{12}$$

Here, $UROT_k$ is defined by:

$$UROT_k = \begin{bmatrix} 1 & 0 \\ 0 & e^{\frac{i\pi}{2^k}} \end{bmatrix} \tag{13}$$

When applied to a two-qubit state $|zk\ zj\rangle$, with the first qubit as the control and the second as the target, $CROT_k$ functions as follows:

- If the control qubit is in state $|0\rangle$, then:

$$\mathrm{CROT}_k \left| 0 z_j \right\rangle = \left| 0 z_j \right\rangle. \tag{14}$$

- If the control qubit is in state $|1\rangle$, then:

$$\mathrm{CROT}_k \left| 1 z_j \right\rangle = |1\rangle \otimes e^{\frac{i\pi z_j}{2^k}} \left| z_j \right\rangle \tag{15}$$

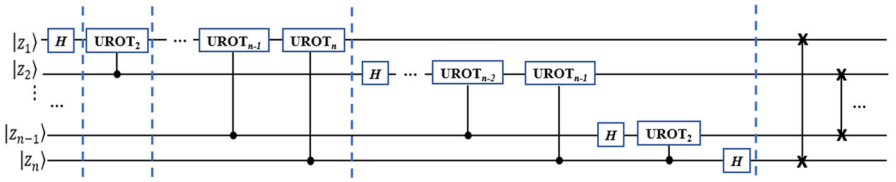

Fig. 3 The QFT for n qubits

These gates, when combined, establish the framework for executing the QFT across an n-qubit system, as depicted in the Fig. 3.

The quantum state, post-encoding, is propelled through the quantum channel, an environment where it is invariably exposed to a spectrum of quantum noise interferences. These interferences are mathematically emulated via quantum gates such as $R_x(\theta)$ and $R_y(\theta)$, which execute rotations around the respective axes of the Bloch sphere by an angle θ. The angle θ serves as a quantitative parameter reflecting the extent of noise within the quantum channel, with larger values of θ denoting increased noise magnitudes.

$$R_x(\theta) = \begin{bmatrix} \cos\left(\frac{\theta}{2}\right) & -i.\sin\left(\frac{\theta}{2}\right) \\ -i.\sin\left(\frac{\theta}{2}\right) & \cos\left(\frac{\theta}{2}\right) \end{bmatrix}$$
$$R_y(\theta) = \begin{bmatrix} \cos\left(\frac{\theta}{2}\right) & -\sin\left(\frac{\theta}{2}\right) \\ \sin\left(\frac{\theta}{2}\right) & \cos\left(\frac{\theta}{2}\right) \end{bmatrix} \tag{16}$$

In the context of Q-OFDM channel, each qubit, post-QFT, experiences a unique rotational transformation, which is randomly selected to be either R_x or R_y. This procedure effectively models the quantum channel's noise by introducing randomness in the phase space of each qubit. Thus, each qubit q_v from the set $\{q_0, q_1, \ldots, q_{n-1}\}$ is subject to a rotation operation $R_{\xi_v}(\theta_v)$, where $\xi_v \in \{x, y\}$ and θ_v is the rotation angle.

The overall channel can be described by a tensor product of these individual operations, which defines the net transformation experienced by the quantum state as it propagates through the channel:

$$U_{\text{channel}} = \bigotimes_{i=0}^{n-1} R_{\xi_v}(\theta_v) \tag{17}$$

The IQFT is designed to reverse the effects of the QFT. It maps a quantum state from the frequency domain, which reveals how often different computational states occur within a quantum state, back to the time or computational basis domain, which describes the state in terms of its position in the computational basis. This process is vital for interpreting the results of quantum computations that have been processed through the QFT.

$$\text{IQFT}|y\rangle = \frac{1}{\sqrt{N}} \sum_{z=0}^{N-1} \omega_N^{-yz} |Z\rangle \tag{18}$$

Acknowledging that ω_N is defined as $e^{\frac{2\pi i}{N}}$ and understanding that N is equal to 2^n, we can accordingly modify the expression to:

$$\text{IQFT}|y\rangle = \frac{1}{\sqrt{2^n}} \sum_{z=0}^{2^n-1} e^{\frac{-2\pi i yz}{2^n}} |z\rangle \tag{19}$$

This equation effectively undoes the QFT, taking the transformed state and reverting it back to its original form before the application of the QFT.The final step in the Q-OFDM system is the measurement process, which is crucial for collapsing the quantum state into a classical bit string.The Q-OFDM process is described as a series of transformations that guide data from its initial state through to its final output, involving stages of encoding, quantum processing, channel influence, decoding, and measurement:

Data is first encoded into a quantum state $|\psi_{enc}\rangle$, then the QFT is then applied, transforming the state to,

$$|\psi_{\text{trans}}\rangle = \text{QFT}|\psi_{\text{enc}}\rangle. \tag{20}$$

The state is affected by the channel that is sent through, resulting in,

$$|\psi_{\text{recv}}\rangle = U_{\text{channel}}|\psi_{\text{trans}}\rangle. \tag{21}$$

IQFT is performed on the received state, yielding,

$$|\psi_{\text{dec}}\rangle = \text{IQFT}|\psi_{\text{recv}}\rangle. \tag{22}$$

Finally, the data is extracted from the quantum state through measurement, giving the output data. These transformations are interlinked, ensuring a smooth transition of data from classical to quantum form and back to classical. Our Q-OFDM model doesn't need to have a cyclic prefix as it does for traditional OFDM systems. This is because quantum mechanics naturally allows for uninterrupted state propagation. This advancement has profound implications for quantum communication systems, offering enhanced efficiency and reliability in the transmission of quantum information.

2.3 BER calculation

In a quantum communication system utilizing a multi-qubit framework, BER is a crucial metric for assessing the reliability and accuracy of information transmission. This system's error performance is quantified by a generalized BER calculation method that accommodates the stochastic nature of quantum channels for systems with varying numbers of qubits [43].

For a given n-qubit quantum state, the procedure commences with the evaluation of BER for every conceivable quantum channel sequence that could influence the state. Here, each qubit is subject to 2 potential transformations, denoted as 'R_x' and 'R_y'.

With this binary transformation scheme, the number of possible channel sequences M_s for an n-qubit state expands exponentially as $\mathrm{M_s} = 2^n$.

$$C_{\text{input, ch}} = \sum_{k=1}^{\text{outcomes}} \sum_{i=1}^{n} \Delta\left(b_i^{\text{expc}}, b_i^k\right) \times \text{ count }_{k,\text{ ch}} \tag{23}$$

where Δ is the Kronecker delta function, b_i^{expc} is the expected bit value, b_i^{k} is the observed bit value, and $\text{count}_{\text{k,ch}}$ is the is the number of times the corresponding outcome was observed of the kth outcome within the specific channel sequence.To calculate the average BER for a single input state across all its channel sequences is:

$$\text{BER}_{\text{average}} = \frac{1}{N_{\text{shots}} \times n \times M_s} \sum_{j=1}^{M_s} C_j \tag{24}$$

This equation reflects the average BER for one input state (0000 for example) across all M_s channel sequences, where C_{j} is the error count for the jth channel sequence. This average is crucial because it represents a consolidation of the BER across the diverse range of channel effects that the state could experience. To clarify, the N_{shots} term accounts for the number of experimental repetitions for each input state and channel sequence to obtain statistical significance in the measurement of the BER. The term n denotes the number of qubits in the system, which determines the complexity of the quantum state. For the overall system BER across all input states and channel sequences, you would then average the BERs calculated for each of the 2^n input states, resulting in:

$$\text{BER}_{\text{system},n\text{qubits}} = \frac{1}{2^n} \sum_{j=1}^{2^n} \text{BER}_{\text{average},j} \tag{25}$$

In this equation, $\text{BER}_{\text{average},j}$ represents the average BER for the jth input state, which is itself an average over all channel sequences and all experimental shots for that state. This provides the overall BER for the system with n qubits, taking into account all possible input states from 0000 to 1111 (for a 4-qubit system, as an example).

3 Simulation results

In the conducted simulation, substantial focus was allocated to the evaluation of the bit error rate (BER) within an OFDM system. The validation of these findings was achieved through comprehensive simulations conducted on the Qiskit platform. Specifically, the simulation employed the quantum simulator known as "qasm_simulator," which is an integral component of the Qiskit Aer package, designed to simulate quantum computing operations.

During the encoding phase of the simulation, message bits are transformed into quantum input states, with binary strings such as '0000' represented as $|0000\rangle$ and

'0001' as $|0001\rangle$, alongside their respective equivalents. This transformation employs a comprehensive look-up table that covers all conceivable n-bit binary strings, facilitating the verification of the states received. The initial quantum state prepared in this manner, which consists of any number between 2 and 8 qubits, is then subjected to a QFT. This critical step transitions the encoded information into the Fourier basis. The simulation operates under the assumption of a uniform probability distribution for the emission of different codewords from the source, a presumption that simplifies the initial analysis framework.

In the Q-OFDM channel scenario, following the QFT, each qubit undergoes a specific rotational transformation, randomly chosen from R_x and R_y. This step effectively emulates the noise characteristics of the quantum channel by introducing variability into the phase space of each qubit. Our model is more general, using uses $R_x(\theta)$ and $R_y(\theta)$ rotations, which represent generalized versions of the depolarizing noise model (where X, Y, and Z gates are used). However, we excluded $R_z(\theta)$ because phase shifts do not affect the measurements used in our simulation. Unlike the depolarizing noise model, which often results in an identity operation, our approach consistently introduces a modification.

For a detailed analysis of channel effects on each input state, the simulation explores every possible sequence and combination of channel operations. For example, with an initial state of '0000', the channel sequence could range from '$R_x\ R_x\ R_x\ R_x$ ' to '$R_x\ R_x\ R_x\ R_y$', and so on, up to '$R_y R_y R_y R_y$'. This comprehensive method allows for an in-depth examination of how channel noise influences the Q-OFDM system, capturing the complexity of noise interactions across the quantum state. These rotations are parameterized by an angle θ, selected from a set of values including 15, 30, 45, and 60°, to simulate a range of channel conditions. In addition, we consider a Gaussian distribution based on a mean of 30° and a standard deviation of 10° for random θ, as shown in Fig. 4.

The process concludes with the application of an inverse quantum Fourier transform (IQFT). The final phase of the simulation involves measurement through a specialized device, thereby facilitating the evaluation of the system's performance, and the process is repeated for a specified number of shots (1024) to gather statistical data.

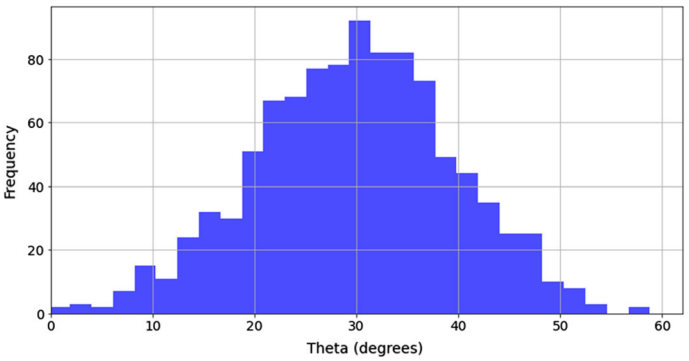

Fig. 4 Histogram of θ values drawn from a Gaussian distribution ($\mu = 30°$, $\sigma = 10°$)

The simulation calculates the BER for each input state across all channel sequences, subsequently deriving the overall system BER for the n-qubit configuration. This includes a thorough consideration of all possible input states, such as '0000' to '1111' for a 4-qubit system, to determine the comprehensive BER across the system. The calculated mean BER provides a metric that reflects the system's performance and robustness, considering both the angle θ and the number of qubits.

In this study, a comparative evaluation was conducted between the quantum OFDM model and a reference model. Both models utilize an identical input stage for encoding quantum states. The Q-OFDM model incorporates QFT and IQFT processes surrounding the channel simulation, whereas the reference model proceeds directly from encoding to channel exposure and subsequent measurement, omitting the QFT and IQFT stages. This comparative approach highlights the Q-OFDM model's distinctive features and evaluates its potential advantages in reducing BER against a conventional backdrop, thereby emphasizing the QFT-IQFT's contribution to quantum communication system performance.

Each data point in the results presented is an average of 10 iterations to ensure statistical reliability and minimize random variations.

In the simulation section, we explore three distinct scenarios to analyze the behavior of the models under various conditions comprehensively:

3.1 Scenario 1: Random θ selection

In this scenario, θ is randomly chosen for both models, adhering to the assumption that, in plausible noise models, θ behaves as an analog random variable, potentially following a Gaussian distribution as shown in Fig. 4. BER is compared between the 2 models to evaluate their performance under these stochastic noise conditions.

Figure 5 illustrates the result of the average BER using both the quantum OFDM model and the reference model with randomly selected values of θ and different numbers of qubits ($n = 2, 3, 4, 5, 6, 7$, and 8). It highlights the superior performance of the quantum model over the reference model, even under stochastic noise conditions. The fluctuations in BER for the reference model across different qubit counts indicate its sensitivity to noise. The quantum model's consistent decline in BER with increasing qubit counts demonstrates its robustness due to the QFT-IQFT stages.

Figure 5 suggests that, within the range of qubit numbers presented, the quantum model outperforms the reference model in terms of BER. For instance, at qubit count 5, the BER in the quantum model is 1.40%, while in the reference model, it is 8.10%. This significant disparity indicates the robustness of the quantum model in mitigating noise through the QFT and IQFT stages.

The noticeable increase in BER for both models at qubit count 5 can be attributed to the broader range of θ values randomly selected, as shown in Fig. 6. The randomly selected θ values for qubit 5 range from 14.4° to 45.3°, while the range for qubit 4 is narrower, between 7.44° and 34.71°. This wider range amplifies noise conditions and increases the BER.

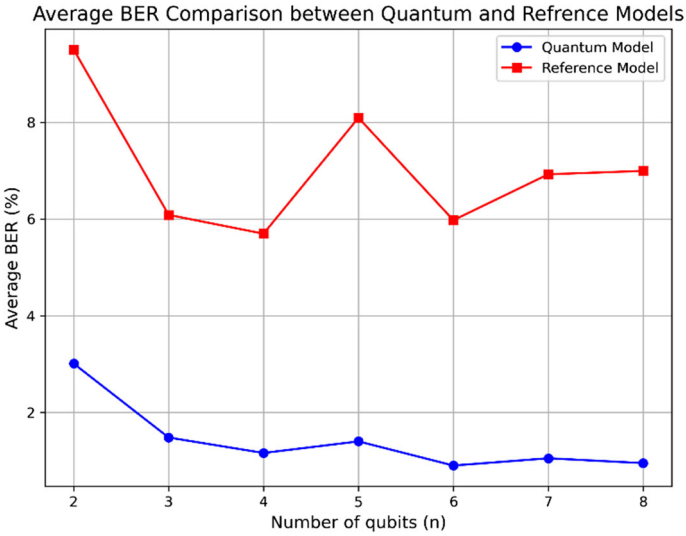

Fig. 5 The avarge bit error rate in different number of qubits in quantum and reference models at random theta selection

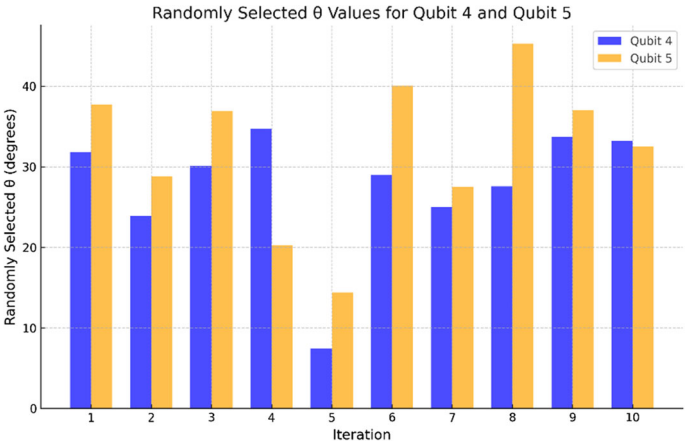

Fig. 6 Randomly selected θ values for qubit 4 and qubit 5

3.2 Scenario 2: Fixed qubit, varied θ

In this scenario, the qubit remains fixed while θ is systematically manipulated across discrete values such as 15, 30, 45, and 60°. This scenario aims to highlight the influence of θ variation on noise amplification and subsequent system performance. The simulation setup involves fixing the qubit count at 4, while varying θ across 15, 30, 45, and 60°.

Figure 7 shows the average BER comparison between the quantum model and the

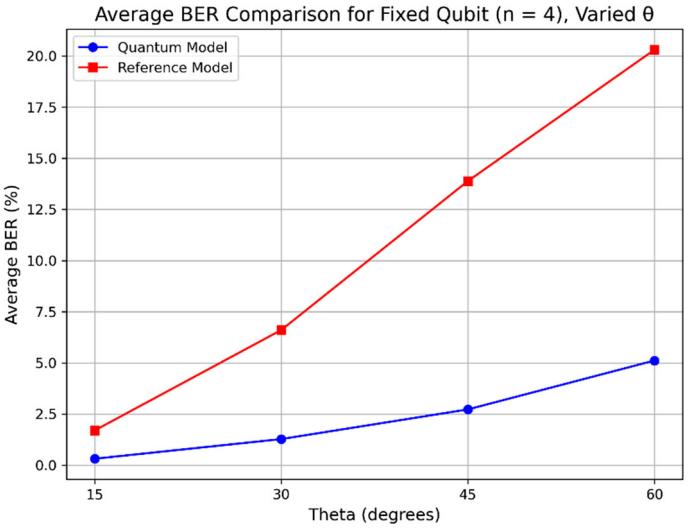

Fig. 7 Average BER comparison between the quantum and reference models with a fixed qubit count ($n = 4$) and varied θ values (15°, 30°, 45°, and 60°)

reference model with a fixed qubit count of 4 while varying θ across discrete values of 15, 30, 45, and 60°. As θ increases from 15 to 60°, both models exhibit an increasing trend in BER due to amplified noise, which is consistent with the expectation that larger angles cause more noise amplification.

The quantum model consistently outperforms the reference model, maintaining a lower BER across all θ values. At $\theta = 15°$, the quantum model has a BER of 0.319%, while the reference model has a BER of 1.7%. At $\theta = 60°$, the quantum model has a BER of 5.12%, compared to 20.31% in the reference model. The difference in BER between the quantum model and the reference model widens as θ increases, illustrating that the quantum model is better at mitigating noise amplification.

3.3 Scenario 3: Fixed θ, changing the number of qubits

In this scenario, θ is held constant at 35° while the qubit count is altered across 2, 3, 4, 5, 6, 7, and 8. The objective is to observe how changes in the qubit count affect the system's output, providing insights into the sensitivity of the models to qubit variations. This setup allows for a detailed examination of each model's response to increased quantum resources, under a consistent angular condition, which is crucial for assessing the scalability and robustness of quantum communication systems.

Figure 8 illustrates the average BER comparison between the quantum and reference models with a fixed θ (35°) and varying qubit counts from 2 to 8. This comparison demonstrates how the BER changes with increasing qubit counts, providing insights into the sensitivity of each model to qubit variations.

The quantum model exhibits a consistent downward trend in BER as the number of qubits increases. This trend is due to the combined effects of QFT and IQFT, which distribute and partially correct errors across qubits. At 2 qubits, the BER for the

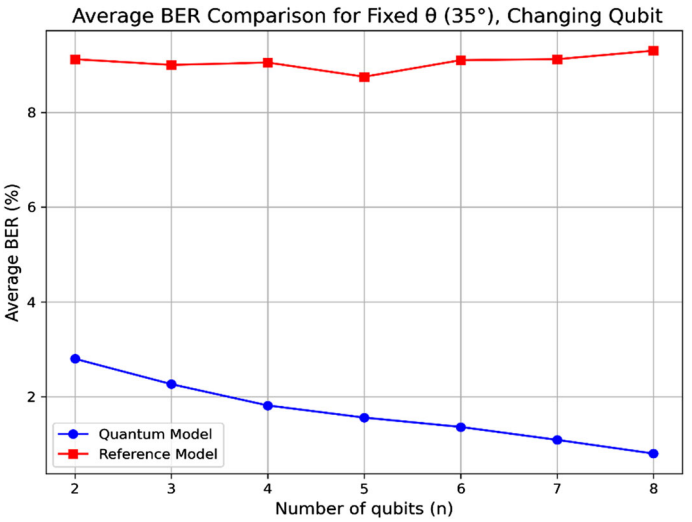

Fig. 8 Average BER comparison between the quantum and reference models for a fixed θ (35°) while varying the qubit count ($n = 2$ to 8)

quantum model is 2.801%. This decreases steadily to 0.8% at 8 qubits, showing the robustness of the model due to error distribution, redundancy through superposition and entanglement, and partial correction through IQFT.

In contrast, the reference model shows a fluctuating trend in BER across varying qubit counts due to the absence of noise-mitigating stages like QFT and IQFT. At 2 qubits, the BER is 9.12%. While the BER decreases slightly to 9.0% at 3 qubits, it fluctuates between 8.75% and 9.3% for qubits 4 to 8, highlighting the sensitivity of the model to errors affecting individual qubits. The reference model does not exhibit a decreasing trend in BER because it lacks the error-distribution, entanglement, and correction mechanisms present in the quantum model. The QFT distributes quantum information and any errors across multiple qubits, reducing the impact of localized errors on overall system performance. Additionally, QFT induces entanglement and superposition, unique quantum states that provide resilience against certain types of errors, effectively lowering the BER as more qubits offer redundancy through shared state information.

After processing through a noisy channel, the application of the IQFT helps to partially undo any errors uniformly spread by QFT, thus recovering the original quantum state more accurately than would be possible without these transforms. However, in the reference model, each qubit carries its segment of information independently without the benefits of QFT and IQFT. This means errors affecting a single qubit can directly influence the measurement output, leading to a fluctuating BER.

The quantum model maintains a significantly lower BER than the reference model across all qubit counts, demonstrating the superior performance of the QFT-IQFT process. The disparity between the 2 models remains substantial as the number of qubits increases. For instance, at 8 qubits, the quantum model achieves a BER of 0.8%, compared to 9.3% in the reference model.

These scenarios collectively offer a comprehensive exploration of the models' performance under different noise conditions, parameter settings, and qubit variations, contributing valuable insights into their robustness and adaptability.

4 Conclusion

This study presents a novel approach to quantum communication through the introduction of quantum orthogonal frequency-division multiplexing (Q-OFDM). By leveraging quantum Fourier transform (QFT) and inverse quantum Fourier transform (IQFT) processes, Q-OFDM offers significant advantages in reducing errors and increasing security in challenging quantum communication environments.

The study is structured around 2 primary models: one incorporating QFT and IQFT, and the other relying solely on a channel comprising randomized rotations (Rx and Ry gates). This dual-model approach facilitates a comprehensive exploration of quantum error dynamics across different circuit configurations. Binary strings were carefully encoded into qubit states, and the resulting bit error rate (BER) was thoroughly analyzed to understand the influence of QFT-IQFT implementation and gate sequence variability on error rates.

The quantum model maintains a significantly lower BER than the reference model across all qubit counts, demonstrating the superior performance of the QFT-IQFT process. The disparity between the 2 models remains substantial as the number of qubits increases. For instance, at 8 qubits, the quantum model achieves a BER of 0.8%, compared to 9.3% in the reference model. As the qubit count rises, only the quantum model shows a reduction in BER, with the quantum model exhibiting a more substantial decline. This pattern highlights the robustness of QFT and IQFT in mitigating errors.

Higher values of θ lead to increased BER in both models. Despite this, the quantum model consistently outperforms the reference model due to error distribution and correction mechanisms inherent in QFT and IQFT. The QFT distributes errors across qubits, while IQFT partially corrects them, reducing the overall impact on system performance. A wider range of θ values leads to greater noise amplification and error distribution.

This research marks a significant advancement in the field of quantum communication by demonstrating the potential of Q-OFDM to enhance communication systems through reduced error rates and increased security. The results indicate that the use of QFT and IQFT stages is crucial for mitigating errors and improving the robustness of quantum communication systems. Future research will focus on exploring sources with varied codeword probabilities, which will further refine the Q-OFDM model and enhance its practicality in real-world quantum communication contexts. Additionally, investigating more complex noise models like the depolarizing noise model and the amplitude damping noise model, as well as advanced error-correcting codes, will help optimize the Q-OFDM system for future quantum networks. This work lays a solid foundation for further exploration and development of secure and efficient quantum communication networks.

Acknowledgements This research was supported by the Ministry of Culture and Innovation and the National Research, Development, and Innovation Office within the Quantum Information National Laboratory of Hungary (Grant No. 2022-2.1.1-NL-2022-00004).

Author contributions Author contributions Abdulbasit Sabaawi: Conceptualisation; formal analysis; investigation; methodology; software; visualisation; writing— original draft. Mohammed Rabeea Almasaoodi: Conceptualisation; formal analysis; investigation; methodology; software; visualisation; writing—original draft. Sandor Imre: Conceptualisation; formal analysis; investigation; methodology; supervision; validation; visualisation; writing—review & editing.

Funding Open access funding provided by Budapest University of Technology and Economics.

Data availability All the data is available in the manuscript.

Declarations

Conflict of interest The authors have no competing interests to declare that are relevant to the content of this article.

Open Access This article is licensed under a Creative Commons Attribution 4.0 International License, which permits use, sharing, adaptation, distribution and reproduction in any medium or format, as long as you give appropriate credit to the original author(s) and the source, provide a link to the Creative Commons licence, and indicate if changes were made. The images or other third party material in this article are included in the article's Creative Commons licence, unless indicated otherwise in a credit line to the material. If material is not included in the article's Creative Commons licence and your intended use is not permitted by statutory regulation or exceeds the permitted use, you will need to obtain permission directly from the copyright holder. To view a copy of this licence, visit http://creativecommons.org/licenses/by/4.0/.

References

1. Imre, S., Balazs, F.: Quantum Computing and Communications: An Engineering Approach. Wiley, Hoboken (2005)
2. Gisin, N., et al.: Quantum cryptography. Rev. Mod. Phys. **74**(1), 145 (2002)
3. Imre, S., Gyongyosi, L.: Advanced Quantum Communications: An Engineering Approach. Wiley, Hoboken (2012)
4. Sabaawi, A.M.A., Almasaoodi, M.R., El Gaily, S., Imre, S.: Energy efficiency optimisation in massive multiple-input, multiple-output network for 5G applications using new quantum genetic algorithm. IET Networks (2023). https://doi.org/10.1049/ntw2.12190
5. Almasaoodi, M.R., Sabaawi, A.M.A., ElGaily, S., Imre, S.: New quantum genetic algorithm based on constrained quantum optimization. Karbala Int. J. Modern Sci. (2023). https://doi.org/10.33640/2405-609X.3325
6. Sabaawi, A., Almasaoodi, M.R., El Gaily, S., Imre, S.: Quantum genetic algorithm for highly constrained optimization problems. Infocommun. J. A Publ. Sci. Assoc. Infocommun. (HTE) **15**(3), 63–71 (2023). https://doi.org/10.36244/ICJ.2023.3.7
7. Gyongyosi, L., Imre, S., Nguyen, H.V.: A survey on quantum channel capacities. IEEE Commun. Surv. Tutor. **20**(2), 1149–1205 (2018). https://doi.org/10.1109/COMST.2017.2786748
8. Quillen, A.C., Skerrett, N.: Generating quantum channels from functions on discrete sets. Quantum Inf. Process. **23**(2), 55 (2024). https://doi.org/10.1007/s11128-023-04254-0
9. Zaman, F., Lee, K., Shin, H.: Information carrier and resource optimization of counterfactual quantum communication. Quantum Inf. Process. **20**(5), 168 (2021). https://doi.org/10.1007/s11128-021-03116-x
10. Liao, S.K., et al.: Satellite-to-ground quantum key distribution. Nature **549**(7670), 43–47 (2017). https://doi.org/10.1038/nature23655

11. Peng, Q., Guo, Y., Liao, Q., Ruan, X.: Satellite-to-submarine quantum communication based on measurement-device-independent continuous-variable quantum key distribution. Quantum Inf. Process. **21**(2), 61 (2022). https://doi.org/10.1007/s11128-022-03413-z
12. Almasaoodi, M.R., Sabaawi, A.M.A., El Gaily, S., Imre, S.: Optimizing Energy Efficiency of MIMO Using Quantum Genetic Algorithm. In: 2023 Advances in Science and Engineering Technology International Conferences (ASET). IEEE, pp 1–6 (2023).
13. Sabaawi, A.M.A., Almasaoodi, M.R., El Gaily, S., Imre, S.: Unconstrained Quantum Genetic Algorithm for Massive MIMO System. In: 2023 17th International Conference on Telecommunications (ConTEL). IEEE, pp 1–6 (2023).
14. Mutreja, S., & Krawec, W. O.: Improved semi-quantum key distribution with two almost-classical users. Quantum Information Processing, 21(9), 319 (2022). https://doi.org/10.48550/arXiv.2203.10567
15. Wehner, S., Elkouss, D., Hanson, R.: Quantum internet: A vision for the road ahead. Science **362**(6412), eaam9288 (2018). https://doi.org/10.1126/science.aam9288
16. Nielsen, M.A., Chuang, I.L.: Quantum Computation and Quantum Information. Cambridge University Press, Cambridge (2010)
17. Li, C.K., Li, Y., Pelejo, D.C., Stanish, S.: Quantum error correction scheme for fully-correlated noise. Quantum Inf. Process. **22**(8), 310 (2023). https://doi.org/10.48550/arXiv.2202.12408
18. Djordjevic, I.B.: Quantum Information Processing, Quantum Computing, and Quantum Error Correction: An Engineering Approach. Academic Press, Cambridge (2021)
19. Swathi, M., Rudra, B.: Novel encoding method for quantum error correction. In: 2022 IEEE 12th Annual Computing and Communication Workshop and Conference (CCWC) (pp. 1001–1005). IEEE, (2022). https://doi.org/10.1109/CCWC54503.2022.9720880
20. Choukroun, Y., Wolf, L.: Deep quantum error correction. arXiv preprint arXiv:2301.11930 (2023). https://doi.org/10.48550/arXiv.2301.11930
21. Hamamreh, J.M., Hajar, A., Abewa, M.: Orthogonal frequency division multiplexing with subcarrier power modulation for doubling the spectral efficiency of 6G and beyond networks. Trans. Emerg. Telecommun. Technol. **31**(4), e3921 (2020). https://doi.org/10.1002/ett.3921
22. Lavanya, P., Satyanarayana, P., Ahmad, A.: Suitability of OFDM in 5G Waveform–A Review. Oriental J. Comput. Sci. Technol **12**(3), 66–75 (2019)
23. Mahmud, M.H., et al.: Performance Analysis of OFDM, W-OFDM and F-OFDM Under Rayleigh Fading Channel for 5G Wireless Communication. In: 2020 3rd International Conference on Intelligent Sustainable Systems (ICISS), Thoothukudi, India, 1172–1177 (2020). https://doi.org/10.1109/ICISS49785.2020.9316134
24. Domínguez-Bolaño, T., et al.: Bit error probability and capacity bound of OFDM systems in deterministic doubly-selective channels. IEEE Trans. Veh. Technol. **69**(10), 11458–11469 (2020). https://doi.org/10.1109/TVT.2020.3011365
25. Abdullahi, M., et al.: A generalized bit error rate evaluation for index modulation based OFDM system. IEEE Access **8**, 70082–70094 (2020)
26. Chen, J., Stoudenmire, E.M., White, S.R.: Quantum Fourier transform has small entanglement. PRX Quantum **4**, 040318 (2023). https://doi.org/10.1103/PRXQuantum.4.040318
27. Nam, Y.S., Blümel, R.: Scaling laws for Shor's algorithm with a banded quantum Fourier transform. Phys Rev A (Coll Park) **87**, 032333 (2013). https://doi.org/10.1103/PhysRevA.87.032333
28. Baaquie, B.E., Kwek, L.-C.: Phase estimation and quantum Fourier transform (qFT). In: Quantum Computers: Theory and Algorithms. Springer, pp 155–169 (2023). https://doi.org/10.1007/978-981-99-0519-1_9
29. Vorobyov, V., Zaiser, S., Abt, N., Meinel, J., Dasari, D., Neumann, P., Wrachtrup, J.: Quantum Fourier transform for nanoscale quantum sensing. NPJ Quantum Inf. **7**, 124 (2021). https://doi.org/10.1038/s41534-021-00457-1
30. Song, D., He, C., Cao, Z., Chai, G.: Quantum teleportation of multiple qubits based on quantum Fourier transform. IEEE Commun. Lett. **22**, 2427–2430 (2018). https://doi.org/10.1109/LCOMM.2018.2871386
31. Mastriani, M.: Quantum Fourier transform is the building block for creating entanglement. Sci. Rep. **11**, 22210 (2021). https://doi.org/10.1038/s41598-021-01745-x
32. Anand, M., Kolusu, P.T.: A novel multi-user quantum communication system using CDMA and Quantum Fourier Transform. In: Ubiquitous Communications and Network Computing: 4th EAI International Conference, UBICNET 2021, Virtual Event, March 2021, Proceedings. Springer, pp 79–90 (2021).

33. Cao, Z., Zhang, C., He, C., Zhang, M.: Quantum teleportation protocol of arbitrary quantum states by using quantum Fourier transform. Int. J. Theor. Phys. **59**, 3174–3183 (2020)
34. Mohammadbagherpoor, H., Oh, Y.-H., Dreher, P., Singh, A., Yu, X., Rindos, A.J.: An improved implementation approach for quantum phase estimation on quantum computers. In: 2019 IEEE International Conference on Rebooting Computing (ICRC). IEEE, pp 1–9 (2019).
35. Bahrani, S., Razavi, M., Salehi, J.A.: Orthogonal frequency-division multiplexed quantum key distribution. J. Lightwave Technol. **33**(23), 4687–4698 (2015)
36. Tanizawa, K., Futami, F.: IF-over-fiber transmission of OFDM quantum-noise randomized PSK cipher for physical layer encryption of wireless signals. J. Lightwave Technol. **40**(6), 1698–1704 (2021). https://doi.org/10.1109/JLT.2021.3119603
37. Kumar, R.: Quantum-enhanced OFDM signal processing: advancing 5G mobile network and IoT communication for healthcare application. Opt. Quant. Electron. **56**(3), 308 (2024). https://doi.org/10.1007/s11082-023-05969-1
38. Yang, X., et al.: DFTs-OFDM based quantum noise stream cipher system. Opt. Fiber Technol. **52**, 101939 (2019)
39. Xu, L., et al.: Resource allocation based on quantum particle swarm optimization and RBF neural network for overlay cognitive OFDM System. Neurocomputing **173**, 1250–1256 (2016)
40. Camps, D., Van Beeumen, R., Yang, C.: Quantum Fourier transform revisited. Numer. Linear Algebra with Appl. **28**(1), e2331 (2021). https://doi.org/10.1002/nla.2331
41. Ruiz-Perez, L., Garcia-Escartin, J.C.: Quantum arithmetic with the quantum Fourier transform. Quantum Inf. Process. **16**, 1–14 (2017)
42. Zhou, S.S., Loke, T., Izaac, J.A., Wang, J.B.: Quantum Fourier transform in computational basis. Quantum Inf. Process. **16**(3), 82 (2017)
43. Eunus, M.E.I, Haque, M.A., Rahman, M S.: Calculation of Bit Error Rates for Superdense and ALOHA based Quantum Communication. In 2021 IEEE International Conference on Telecommunications and Photonics (ICTP) (pp. 1–4). IEEE, (2021).

Publisher's Note Springer Nature remains neutral with regard to jurisdictional claims in published maps and institutional affiliations.